IMPROVED INTERMEDIATE-DISTANCE PHASE CHARACTERIZATION IN CENTRAL ASIA

Delaine Reiter, Aaron Ferris, and Michelle Johnson

Weston Geophysical Corporation

Sponsored by Air Force Research Laboratory

Contract No. FA8718-06-C-0002

ABSTRACT

Accurate knowledge of waveform characteristics observed at far-regional and near-teleseismic distances is critically important for regions in which arrays are sparsely located. Significant body-wave phase complexities that are observed at distances between 13-30°. These complexities produce uncertainties in phase identification and errors in phase arrival-time estimation. Our research project focuses on two principal tasks designed to improve the identification and characterization of body-wave phases observed at intermediate distances in Central Asia.

In the first task we are investigating array-processing techniques to improve estimates of phase arrival times, amplitudes, slownesses and back azimuths from events at intermediate distances. At epicentral distances of 13-30° seismic waves interact with upper mantle discontinuities, and multiple body-wave arrivals often occur over 4-20 second time windows on the seismogram. To enhance and distinguish between these multiple arrivals of similar frequency content, we are investigating the capabilities of vespagram, semblance-stacking, MUltiple Signal Classification (MUSIC) and cross-correlation techniques. We are extensively testing and validating these algorithms to determine the optimum detection and identification procedures to use on observed data. Our primary data sources are the Kazakhstan regional arrays in Makanchi (MKAR) and Karatau (KKAR).

In our second task we have begun a study of the seismic velocity and discontinuity structure beneath Central Asia. Accounting for known seismic heterogeneity will allow us to more accurately predict the travel-time characteristics of intermediate-distance body-wave phases, which in turn will help us to distinguish between poor phase identification and path-related behavior at these distances. We are collecting and reconciling previously published receiver-function models for stations in our study area. We plan to append several of the available global upper-mantle models to the base of these receiver functions and use the resulting 1-D velocity models in full-waveform synthetic studies.

OBJECTIVES

This project is focused on improving body-wave seismic phase characterization at far-regional and near-teleseismic distances. At distances of approximately 1500-2800 km from a seismic event, propagation complexities arise that cause significant difficulties in the interpretation of seismograms. At these distances seismic waves sample upper-mantle low-velocity zones (LVZ) and discontinuities at approximately 410 and 660 km depth. This interaction results in triplications and interference phenomena in wave propagation, which consequently produce uncertainties and errors in bulletin phase picks. We demonstrate this phenomenon in Figure 1a, in which we plotted *Pn/P* travel-time residuals as a function of epicentral distance. To generate this figure, we retrieved the International Seismological Centre (ISC) bulletins for the years 1999-2001 from the Flinn-Engdahl Seismic Regions 26-30, 47 and 48 (see http://neic.usgs.gov/neis/epic/fer.html), which include most of Asia and areas of the Middle East. We filtered this data set to include all events with ISC depths less than 40 km that were located by more than 25 stations. In Figure 1a, we plotted the residuals (gray dots) with respect to the IASPEI91 global 1D model (Kennett and Engdahl, 1991) for associated, first-arriving *P*-wave picks between 10-30°. Then we calculated the density (number) of residual picks in boxes of 0.5° by 0.5 seconds and superposed a smoothed version of the resulting image over the individual picks. The two dashed black lines show the travel-time differences between branches *C'B'- A'B'* and *CB - AB* in Figure 1b, which depicts the *iasp91* travel-time curves for upper-mantle arrivals.

Figure 1a clearly shows a high-density region of travel-time residuals that are associated with the 410-km phase triplication (occurring at 14-18° epicentral distance). There is also considerable structure to the residuals in the regional to far-regional range, revealed by the negative bias of residuals at distances between 10-17°. While this particular data set does not reveal an increase in phase residuals associated with the 660-km discontinuity (i.e., the *CB* travel-time branch), we have observed such an effect for other time ranges and in other bulletins (e.g., the National Earthquake Information Center [NEIC]). This type of residual behavior as a function of epicentral distance is also present in the phase picks used to locate events at the ISC (i.e., the time-defining phases), but other agencies restrict their location travel-time picks more aggressively, making the phenomenon shown in Figure 1a less apparent.

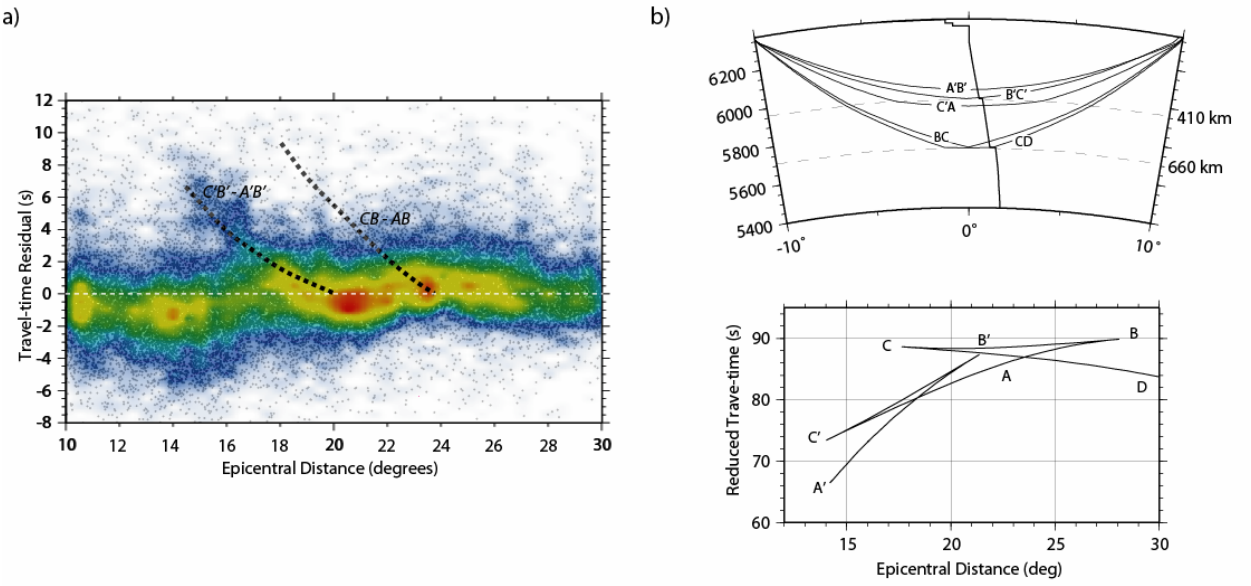

Figure 1: a) Associated *P/Pn* phase residuals (with respect to the global 1D *iasp91* model) from ISC bulletins in Asia (1999-2001) as a function of epicentral distance. Heavy black dashed lines show the travel-time difference between secondary and primary upper-mantle phase branches of the *iasp91* travel-time curves. b) Ray-path illustrations (top) and reduced travel times (bottom) for phases that sample upper-mantle discontinuities at 410 and 660 km depths. The two predominant triplication effects from this set of arrivals occur at distances between approximately 14-18° and 20-24°.

The variation of the residuals shown in Figure 1 illustrates the fundamental question we wish to address in our research project: What are the causes of heterogeneous behavior in travel-time residuals at the distance range between 13-30°? There are likely to be two primary causes for the residuals shown in Figure 1: 1) phase misidentification and 2) unaccounted-for crustal and upper-mantle heterogeneity. In our study, we are quantitatively examining the causes of phase residuals and uncertainties at these distances, trying to determine whether they might be due either to poor phase identification or upper-mantle heterogeneity (or both). Our goal is to ensure that the techniques and results developed will be directly applicable to the regional monitoring problem.

Thus, our research objectives focus on 1) array-processing techniques capable of distinguishing between closely-spaced arrivals; and 2) studies of upper-mantle heterogeneity between 150-700 km depths at intermediate distances from arrays and stations in Central Asia. The results of these studies will produce a methodology to characterize body-wave phases in Central Asia observed at intermediate distances using small-aperture arrays. Our deliverables will also include 'templates' of typical events and associated phase behavior, supported by accurate velocity models, in specific regions such as Iran, Turkmenistan, Pakistan, northern India, and western China.

RESEARCH ACCOMPLISHED

The objective of our research project is a better understanding of the behavior of primary and secondary body-wave arrivals at distances between 13-30°, which will lead to more accurate location and discrimination efforts, particularly for small events. Therefore, we are studying ways to improve the identification and characterization of phases at intermediate distances observed in Central Asia. We believe that a study of this type will help to reduce the uncertainties currently associated with phases observed at these distances.

To address the phase misidentification problem, we are developing array-based methods that can differentiate between closely-spaced arrivals in the seismogram. The use of arrays has the potential to reduce phase misidentification, primarily because of the greater confidence in the phase analysis that multiple recordings of a very similar wavefield provide. Array methods allow seismologists to resolve subsurface features at a finer scale and examine waveform features in great detail with more confidence. However, there is a significant complication with array observations at intermediate distances, in that the small aperture of current regional arrays is poorly designed to resolve small slowness variations in the early *P*-wave coda. Our research will address this complication through the development and adaptation of array methods to our specific problem.

To address the problem of seismic velocity heterogeneities as they pertain to understanding phase arrivals at intermediate epicentral distances, we have begun a study of the crust and upper-mantle velocity (and discontinuity) structure in the regions surrounding the MKAR and KKAR regional arrays in Kazakhstan. There is an extensive body of previous research on tectonic and seismic structure in the broad region surrounding Kazakhstan that we can draw upon, but we will augment the previous research by closely examining the velocity structure in the mantle from ~400-700 km depths and the seismic phases that sample that structure.

We are applying the array techniques we develop to data from Central Asia. For the current project, we will concentrate on the available data from the small-aperture arrays in MKAR and KKAR, which have been reporting since 2002 and early 2003 for MKAR and KKAR, respectively. Figure 2 shows the location of the MKAR and KKAR arrays as well as the abundant seismicity (from the 1973-2004 NEIC bulletins) at distances between 13-30° from each array. The pink and blue annular regions surrounding each array are simple cartoons of the surface region where intermediate-distance phases bottom before arriving at MKAR or KKAR.

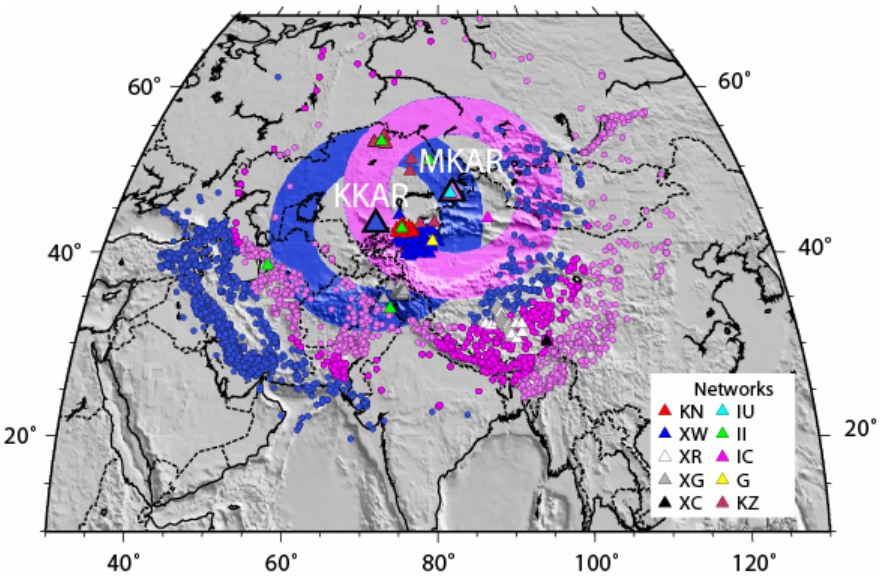

Figure 2. Map of the study region and US AEDS arrays (MKAR and KKAR) in Central Asia. Earthquakes at intermediate distances from the arrays (from the 1973-2004 NEIC bulletins) are plotted, with annular regions showing the surface expressions of upper-mantle transition zones sampled by the earthquakes. Also plotted are the open networks and stations in the region (available from the Incorporated Research Institutions for Seismology [IRIS]).

MKAR/KKAR Earthquake Database

To provide a test bed for our analysis techniques, we are collecting data from moderate-sized events observed at the MKAR and KKAR arrays. We populate the database with events that are well located teleseismically and have Harvard Centroid Moment Tensor (CMT) solutions (Dziewonski et al., 1981) associated with them. To date we have collected waveforms for 198 earthquakes appearing in the EHB (Engdahl et al., 1998) bulletin, comprised of 83 KKAR and 115 MKAR recordings. Figure 3 shows the event locations of our current earthquake database. We note that all of the events currently in the data set were observed at distances between 14-18° from at least one of the arrays, since we intend to focus our initial studies on the 410-km mantle discontinuity.

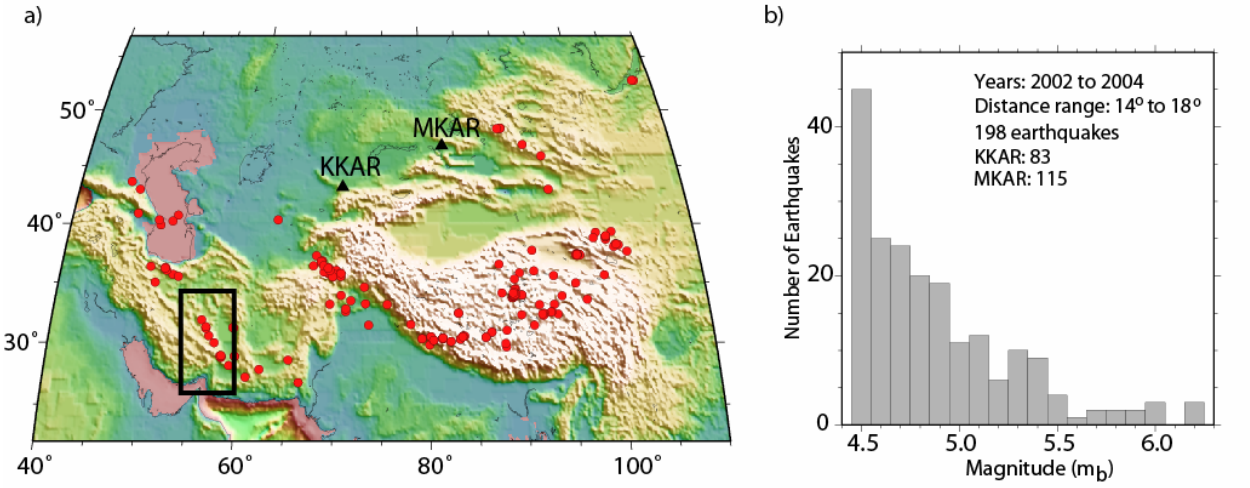

Figure 3. a) Distribution of our current test-bed database of earthquakes at intermediate distances from MKAR and/or KKAR. b) Histogram showing the magnitude distribution of the database (all events have Harvard CMTs associated with them).

To illustrate the waveform variability we see in our data set, Figure 4 displays a record section from several southern Iran earthquakes (m_b ~ 4.5-6.0) recorded at the KKAR array. The black box in Figure 3 outlines the location of the events shown in Figure 4. Each vertical-component waveform in Figure 4 is aligned on the analyst-picked *P* arrival and filtered between 0.1 – 1.75 Hz. We note that most of the *P* arrivals are emergent, and while there are indications of similarities in the secondary arrivals, the waveforms do not reveal any strong overlapping characteristics. Since these events are observed at KKAR inside a small epicentral and azimuthal range, it will be necessary to extract considerable information about the sources, path structure, and event locations in order to make some conclusions about the body-wave phases seen at the arrays and nearby broadband stations.

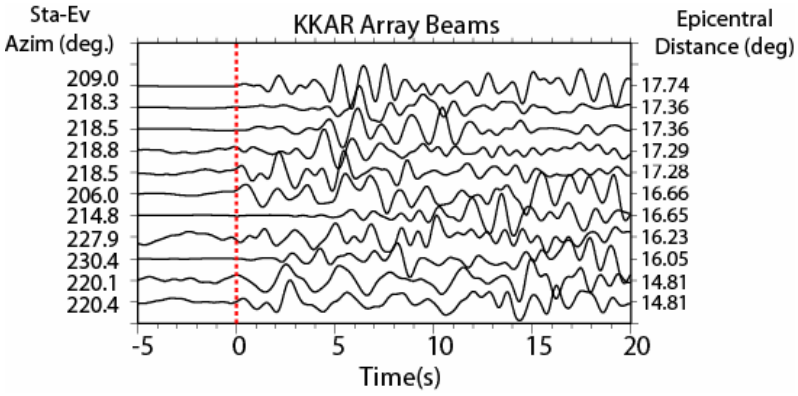

Figure 4. Waveform section showing the KKAR array beams from earthquakes inside the orange box in Figure 3a. All waveforms have been aligned on their direct *P*-wave arrival time from the EHB bulletin. Note that even though the events are arriving from a tight back azimuth and epicentral distance range at KKAR, they exhibit significant variation in their initial arrivals.

Array-Processing Techniques for Improved Intermediate-Distance Phase Characterization

To improve phase characterization at far-regional and near-teleseismic distances, we will need analysis techniques that can separate closely-spaced arrivals related to transition-zone discontinuities. We are examining the capabilities of array-based techniques such as vespagram, improved frequency-wavenumber (*f-k*), and cross-correlation, all of which can produce accurate estimates of phase travel times, azimuths, and slownesses.

For example, there are many classical and recently improved *f-k* techniques available from the technical literature. We are developing a version of the MUSIC estimator (Schisselé et al., 2004), which utilizes a continuous wavelet transform (CWT) to help identify the time windows in which coherent phases exist. Once the user has defined this window, the MUSIC estimate returns estimates of the propagation characteristics of the analyzed phase.

Another analysis technique that may hold promise for triplicated phase arrivals is a modification of a traditional vespagram (the velocity spectral method, also known as the 'slant-stack' method). Vespagrams display seismic signals recorded at an array in terms of the energy content of the incoming signal as a function of the slowness (Davies *et al.*, 1971). Vespagram analysis is used in diverse applications, including mapping transition-zone discontinuities in the Pacific using precursors to *PP* (Rost and Weber, 2002) and processing small events from mines in northwestern Russia (Gibbons and Kvaerna, 2002). In traditional vespagram analysis, the energy in the array data is displayed as a function of horizontal slownesses and back azimuth. However, the linear vespagram cannot always resolve arrivals that have very similar slownesses. To address this, the n^{th} -root vespagram (Muirhead and Datt, 1976) takes the n^{th}-root (n=2,3,4,…) of the amplitudes of all array traces prior to performing the slant-stack or vespagram calculation.

To illustrate the methods described above, we analyzed an event in Tibet that was observed at the MKAR and KKAR arrays. Figure 5a shows the location of the Kazakhstan arrays, as well as the Harvard CMT solution for the event, which occurred at the edge of the Tibetan Plateau (Qinghai, China). In Figure 5b we display the 1D *P* and *S* velocity model we used to predict P-wave travel times using the Tau-P Toolkit (Crotwell et al., 1999). This velocity model is a composite profile derived from the CRUST2.0 model (Bassin et al., 2000) and the IASPEI91 1D

reference model (Kennett and Engdahl, 1991) mid-way between the arrays and the event. Figure 5c shows the first 20-40 seconds of unfiltered short-period data from the nine-element MKAR and KKAR arrays, which observed the event at distances of 14.11° and 20.54°, respectively. Table 1 provides event location and magnitude information extracted from several seismic bulletins.

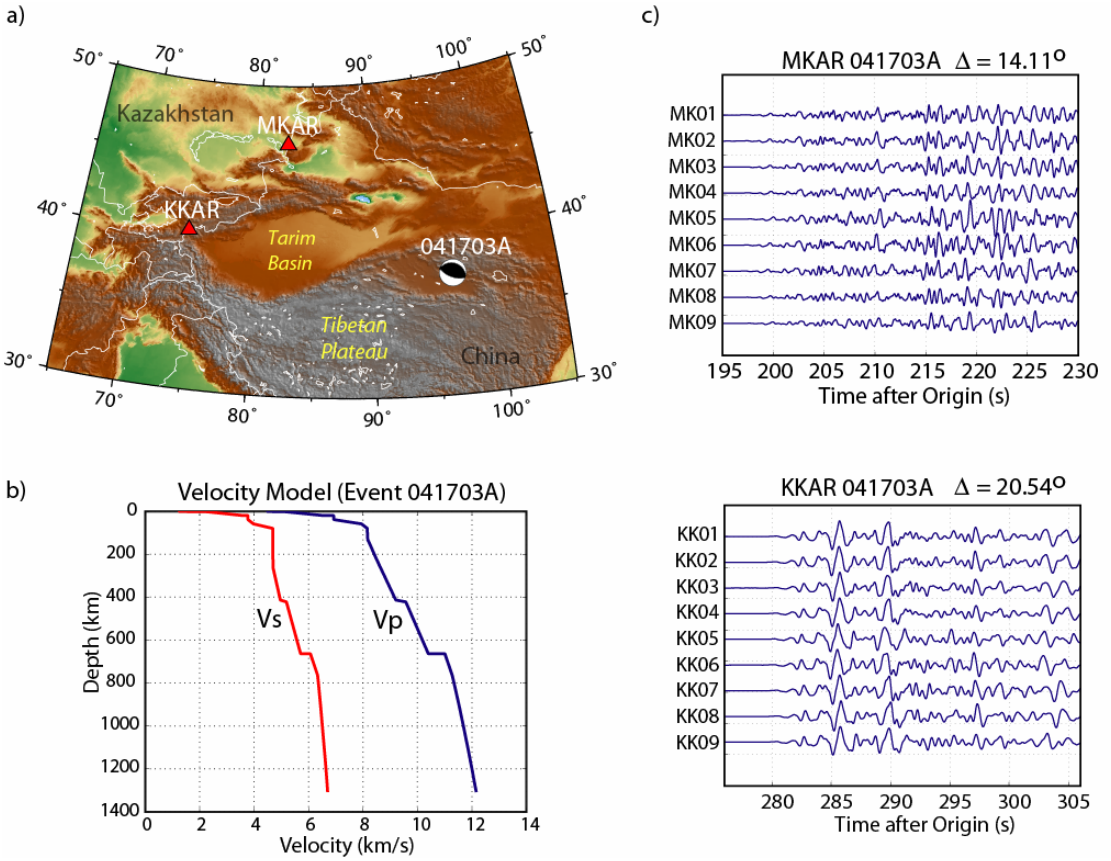

Figure 4. Event in Tibet (EVID 041703) used to illustrate analysis techniques. a) Regional map including event and array locations and the published Harvard CMT solution; b) 1D velocity model used to predict the travel times of triplicated *P* phases; and c) MKAR and KKAR array gathers recorded for the event.

Table 1. Location and magnitude information from several agencies for the Tibetan event shown in Figure 5.

Event 041703 Origin Parameters					
Agency	**Origin Time**	**Latitude**	**Longitude**	**Depth (km)**	**Magnitude**
IDC	00:48:38.09	37.52	96.67	0.0f	5.7 (mb)
NEIC	00:48:38.58	37.53	96.48	14.0f	6.4 (MW)
HRVD	00:48:46.30	37.53	96.45	16.0	6.2 (mb)
ISC	00:48:38.63	37.52	96.51	15.0f	6.2 (mb)

Figure 6 shows results from applying both MUSIC and vespagram analysis to the KKAR recordings of Event 041703. In Figure 6a, we show the 1st-root (i.e., classic slant-stack) vespagram of the unfiltered array data beneath the KKAR array beam. In both figures, the array beam was calculated using the predicted *P*-slowness from the IASPEI9*1* model (Kennett and Engdahl, 1991) and the back azimuth from the ISC event location. The results clearly illustrate the difficulties in resolving the phase arrival velocity at small-aperture arrays with the classic vespagram

method. To confidently identify the different triplicated *P* arrivals from the upper mantle, we need phase velocity resolution on the order of ~0.5 km/s.

In Figure 6b, we show the results from applying the MUSIC estimator to arrival P2 shown in the top subplot of the array beam. The results indicate that the MUSIC technique estimates a well-constrained phase velocity that corresponds to the *P660* arrival time predicted by the IASPEI91 model. From these initial results, we can see that the MUSIC estimator shows promise; however, the classic vespagram method requires further enhancement.

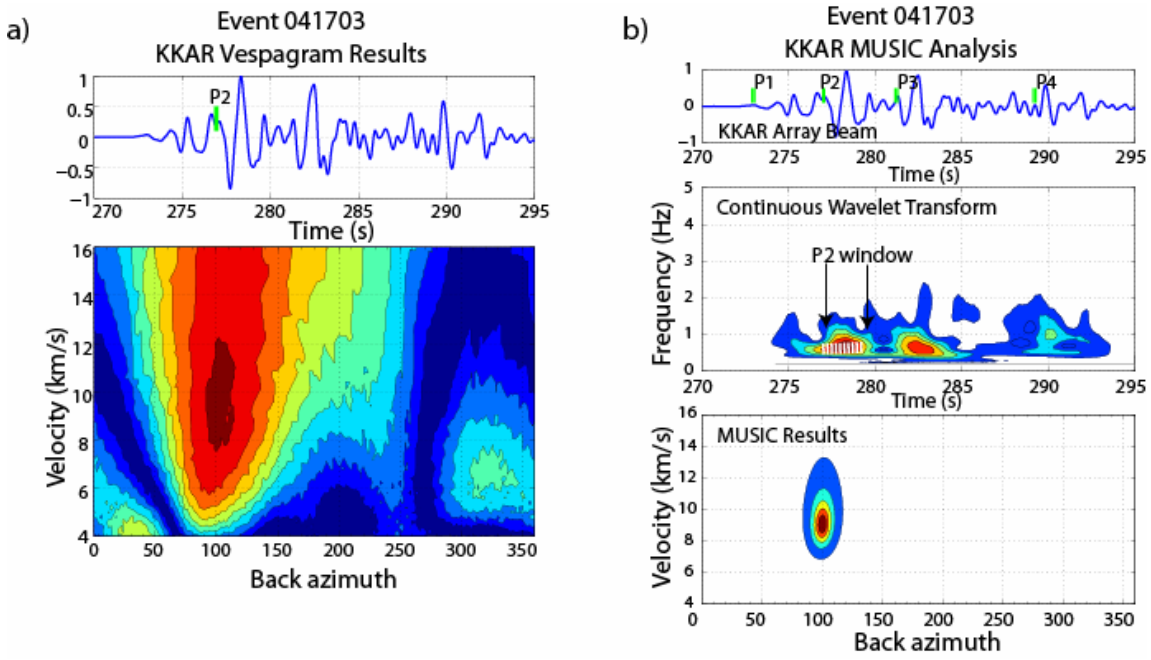

Figure 5. a) KKAR array beam for Event 041703 (top) and single-root (or classical slant-stack) vespagram analysis (bottom) applied to large-amplitude arrival P2; b) KKAR array beam (top), continuous wavelet transform (middle) and MUSIC estimator (bottom) applied to the P2 window outlined in white in the wavelet transform subplot. The results show that the classical vespagram technique does not have the slowness resolving power of the MUSIC estimation technique.

To address the deficiency in the classical vespagram analysis, we are developing modifications that can be used to better quantify the wave propagation characteristics. For example, Figure 7 shows the 4^{th}-root vespagram analysis for a 4-second window that includes 2 seconds of the initial *P* phase at the KKAR array (Figure 7a). Even though we applied the 4^{th}-root vespa process, the phase-velocity is still not well-resolved. In this case, the vespa process incorrectly estimates a phase velocity of 32.5 km/s for this arrival (shown as the orange dot in Figure 7b), whereas the theoretical phase velocity is 10.2 km/s. This lack of slowness resolution is an inherent obstacle in analyzing events at intermediate distances using small-aperture arrays and classical methods. However, an examination of the gradient of the vespa amplitude versus phase velocity shows a maximum gradient change at 9.7 km/s. This is remarkably near the theoretical phase velocity of 10.2 km/s (Figure 6c). This preliminary observation suggests that an enhanced vespagram method, which takes into account the gradient of the vespa amplitude, might be able to increase the slowness resolution of arrivals from intermediate-distance events.

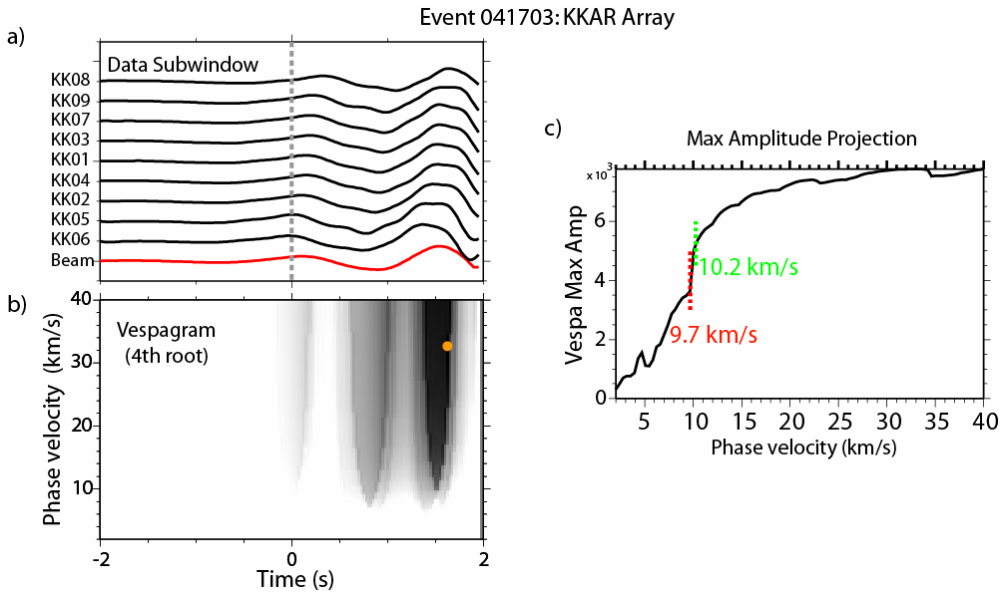

Figure 6. a) Sub-windowed KKAR data from the initial *P*-wave phases. The *P* arrival at the closest station is aligned to zero-offset (dashed line), and the best beam resulting from the vespa analysis is shown in red. b) Vespagram (4th-root) of the signals shown in (a). Gray scale represents the beam power for different stacking velocities. The orange dot marks the phase velocity that produces the best beam (red waveform in a). c) A projection of the vespa image along ~1.6 sec showing the variation of vespa amplitude to phase velocity. The green dashed line marks the theoretical *P*-wave phase velocity, and red dashed line marks the maximum gradient in slope along the projection.

Upper-Mantle Structure Studies Using Full-Waveform Modeling

There are abundant sources of data in central Asia for the study of phase characterization through waveform modeling. In China and northern India, there have been many experiments and resulting studies of the tectonics and seismic velocity structure. A few of the relevant experiments include the INDEPTH experiment (International Deep Profiling of Tibet and Himalaya; 52 seismographs deployed across central Tibet; Zhao et al., 1993), and experiments in Nepal/Tibet (Schulte-Pelkum et al., 2005) and Pakistan (Meltzer et al., 1996).

In countries of the Former Soviet Union, temporary experiments around the Caspian Sea and permanent regional networks such as KNET in the Tien Shan of Kyrgystan have produced data and regional velocity models to describe wave propagation (e.g., Ghose et al., 1998; Martynov et al., 2004). There are also several in-country networks (for example, in Turkmenistan and Uzbekistan) that provide their data to IRIS; the data from these networks could be used to provide important constraints on the seismic velocity structure in the surrounding regions.

We are compiling pre-existing information on the lithospheric and upper-mantle structure in our study region that has a direct bearing on the phase characterization from events at intermediate epicentral distances. This includes information regarding crust and upper-mantle velocity structure, such as the sub-vertical velocity high below Tibet that may document the down-welling of the Indian mantle lithosphere beneath Tibet (Tilmann et al., 2003), as well as the 20-km topographic change in the 410-km discontinuity across the Kazakh shield and the Tien Shan. Incorporating information such as in these two examples will be crucial in understanding the effects of mantle heterogeneity on phase arrivals from intermediate-distance events.

Many receiver function (RF) studies have been performed in our region, for stations in Iran (Hatzfeld et al., 2003), northeastern India and Tibet (Mitra et al., 2005), and the Tien Shan in Kyrghystan (Bump and Sheehan, 1998; Oreshin et al., 2002), among many others. RF analysis is used to determine the crust and upper mantle structure immediately beneath three-component broadband stations. The resulting velocity structure is based on modeling the amplitudes of *P* to *S* conversions and their reverberations in teleseismic *P*-wave coda, following deconvolution of the vertical component from the radial and transverse components of broadband data. We are concentrating on RF

models, because information about the discontinuity structure provided by these models may prove to be more useful in phase characterization than models from tomographic studies. We have gathered the available literature detailing RF-based models from previous studies. Figure 7 shows the RF station coverage we have discovered to date in the literature; we have started to compile these models and compare them to the other regional velocity models that are available for the crust and upper mantle. Following this exercise we will supplement our collection of RF models wherever we have gaps in our coverage, using available data from stations within the circular regions shown in Figure 2.

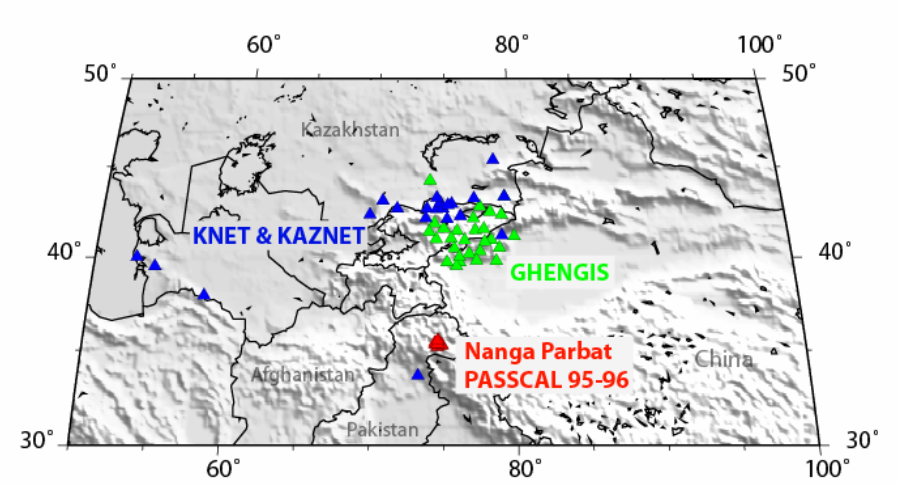

Figure 7. The stations (triangles) indicate locations where a receiver-function model in our study region has been published in the seismological literature. We are collecting the models for the purpose of full-waveform modeling to improve phase characterization of the early portion of the *P* waveform at intermediate distances.

As have other researchers (Rodgers and Schwartz, 1998; Leborgne et al., 1999), we will initially focus on developing representative 1D models for paths of interests. We will not create new models of the transition-zone structure, since other researchers have published in-depth studies of the mantle transition zones in our region. We will instead derive models of the transition zone from published 1D and 3D mantle models. These mantle models will be appended to the high-resolution crust and uppermost mantle RF models to create path-appropriate composite 1D models, and the results used for synthetic waveform generation.

We will generate waveform synthetics using the 1D reflectivity (Kennett, 1988) method. Our primary goal will be to explain the phase travel-time behavior observed at the MKAR and KKAR arrays. It is likely that, rather than modeling random events, we will collect and identify 'templates' of typical events and associated phase behavior, supported by accurate velocity models, in specific regions such as southern Iran, Turkmenistan, Pakistan, northern India, and western China.

CONCLUSIONS AND RECOMMENDATIONS

Our study of intermediate-distance phase characterization will accomplish two important nuclear monitoring objectives. First, we are developing and testing array-based techniques that will improve the identification of closely-spaced phases observed at intermediate epicentral distances. So far, no comprehensive array-based approach has been attempted (by either the national laboratories or the external research community) to resolve the difficult problem of identifying seismic phases in this important distance range. These techniques will be a strong contribution from the project that could be applied to other array data and monitoring applications.

We are also developing information and associated results on transition-zone velocity and discontinuity structure in Central Asia. This information will distill and augment the results from previous and ongoing tectonic studies of the region. While many studies have focused on crust and mantle structure for the upper 200 km in central Asia, we will perform full-waveform modeling using composite models that include additional transition-zone structure at depths between 400-700 km. It is this deeper structure (in conjunction with accurate models between the surface and ~250

km) that has the strongest effect on the succession of phases observed at distances of 13-30°. In summary, our efforts to combine array-based signal processing and waveform modeling to better understand complex phase behavior should in turn lead to better event location and discrimination capabilities at lower magnitudes.

REFERENCES

Bassin, C., G. Laske and G. Masters (2000). The Current Limits of Resolution for Surface Wave Tomography in North America, *EOS Trans AGU*, 81, F897.

Bump, H. A., and A. F. Sheehan (1998). Crustal thickness variations across the northern Tien Shan from teleseismic receiver functions, G*eophys. Res. Ltrs.* 25: 1055–1058.

Crotwell, H.P., T.J. Owens, and J. Ritsema (1999). The TauP Toolkit: Flexible seismic travel-time and raypath utilities, *Seis. Res. Ltrs.* 70: 15–170.

Davies, D., E. J. Kelly, and J. R. Filson (1971). Vespa process for analysis of seismic signals, *Nature Phys. Sci*. 232: 8–13.

Dziewonski, A.M., T.-A. Chou and J.H. Woodhouse (1981). Determination of earthquake source parameters from waveform data for studies of global and regional seismicity, *J. Geophys. Res*. 86: 2825–2852.

Engdahl E. R., R. van der Hilst, and R. Buland (1998). Global teleseismic earthquake relocation with improved travel times and procedures for depth determination, *Bull. Seism. Soc. Amer*. 88: 722–743.

Ghose, S., M. W. Hamburger, and J. Virieux (1998). Three-dimensional velocity structure and earthquake locations beneath the northern Tien Shan of Kyrgyzstan, central Asia, *J. Geophys. Res.*: 103: 2,725–2,748.

Gibbons, S., and T. Kvaerna (2002). Analysis and processing of events from the Kovdor Mine, Kola, NW Russia, *NORSAR Contribution 793*, http://www.norsar.no/seismology/research/kovdor/kolareport.pdf.

Hatzfeld, D., M. Tatar, K. Priestley, and M. Ghafory-Ashtiany (2003). Seismological constraints on the crustal structure beneath the Zagros Mountain belt (Iran), *Geophys. J. Int.* 155: 403–410.

Kennett, B. L. N., and E. R. Engdahl (1991). Travel times for global earthquake location and phase identification, *Geophys. J. Int*. 105: 429–465.

Kennett, B.L.N. (1988). *Systematic Approximations to the Seismic Wave Field*, Chapter III.1 in Seismological Algorithms**,** ed. D.J. Doornbos, Academic Press.

Leborgne, S., and R. Madariaga (1999). Body waveform modeling of east Mediterranean earthquakes at intermediate distances (17-30) with a Gaussian beam summation method, *J. Geophys. Res*. 104: 28,813–28,828.

Martynov, V. G., F. L. Vernon, D. L. Kilb, and S. W. Roecker (2004). Directional variations in travel-time residuals of teleseismic *P* waves in the crust and mantle beneath Northern Tien Shan, *Bull. Seis. Soc. Amer* 94: 650–664.

Meltzer, A. S., P. K. Zeitler, M. L. Schoemann, B. C. Beaudoin, L. Seeber, and J. G. Armbruster (1996). The Nanga Parbat Seismic Experiment, *Eos Trans. AGU (Supplement)* **77**: 688.

Mitra, S., K. Priestley, A. K. Bhattacharyya, and V. K. Gaur (2005). Crustal structure and earthquake focal depths beneath northeastern India and southern Tibet, *Geophys. J. Int.* 160: 227–248.

Muirhead, K. J., and R. Datt (1976). The N-th root process applied to seismic array data, *Geophys. J. R. Astron. Soc*. 47: 197–210.

Oreshin, S., L. Vinnik, and D. Peregoudov (2002). Lithosphere and asthenosphere of the Tien Shan imaged by *S* receiver functions, *Geophys. Res. Ltrs.* 29: doi:10.1029/2001GL014441.

Rodgers, A. J., and S. Y. Schwartz (1998). Lithospheric structure of the Qiangtang Terrane, northern Tibetan Plateau, from complete regional waveform modeling: Evidence for partial melt, *J. Geophys. Res*. 103: 7,137–7,152.

Rost, S., and M. Weber (2002). The upper mantle transition zone discontinuities in the Pacific as determined by short-period array data, *Earth Planet Sci. Ltrs.* 204: 347–361.

Schisselé, E., J. Guilbert, S. Gaffet, and Y. Cansi (2004). Accurate time–frequency–wavenumber analysis to study coda waves, *Geophys. J. Intl*. 158: (2), 577–591.

Schulte-Pelkum, V., G. Monsalve, A. Sheehan, M. R. Pandey, S. Sapkota, R. Bilham, and F. Wu (2005). Imaging the Indian subcontinent beneath the Himalaya, Nature, 435, 1,222–1,226.

Tilmann, F., J. Ni and the INDEPTH II Team (2003). Seismic Imaging of the Downwelling Indian Lithosphere Beneath Central Tibet, *Science*, 300: (5624), 1424–1427, DOI: 10.1126/science.1082777 .

Zhao, W., K. D. Nelson, and the Project INDEPTH Team (1993). Deep seismic reflection evidence for continental underthrusting beneath southern Tibet, *Nature* 366: 557–559.